A Novel Nonairon(III) Citrate Complex: A "Ferric Triple-Decker"

Avi Bino,*,[1a] Itzhak Shweky,[1a] Shmuel Cohen,[1a] Erika R. Bauminger,[1b] and Stephen J. Lippard*,[1c]

Department of Inorganic and Analytical Chemistry and Racah Institute of Physics, The Hebrew University of Jerusalem, 91904 Jerusalem, Israel, and Department of Chemistry, Massachusetts Institute of Technology, Cambridge, Massachusetts 02139

The novel nonairon(III) citrate complex $[Fe_9O(cit)_8(H_2O)_3]^{7-}$ (**3**) [cit = $C(O^-)(COO^-)(CH_2COO^-)_2$] was prepared as its neocuproinium salt by reacting ferric nitrate, sodium citrate, and neocuproine (neo; 2,9-dimethyl-1,10-phenanthroline) in a 1:1:1 ratio in aqueous solution. The compound $(Hneo)_7 \cdot \mathbf{3} \cdot neo \cdot 61H_2O$ crystallizes in the monoclinic space group $P2_1/c$ with unit cell parameters of $a = 21.910(3)$ Å, $b = 25.788(5)$ Å, $c = 39.653(6)$ Å, $\beta = 99.47(1)°$, $V = 22\,099(7)$ Å^3, and $Z = 4$. The anionic complex consists of three parallel triangular Fe$_3$ units, 5.6 Å apart, forming a slightly distorted trigonal prism. The outer two units are connected by three bridging tetradentate cit^{4-} ligands to the central one, and each of the terminal Fe$_3$ units is capped by another cit^{4-} ligand. The central Fe$_3$ unit has the oxo-bridged basic iron carboxylate structure, whereas the two terminal ones have a "voided cubane" structure with an $\{Fe_3O_4\}$ core. Mössbauer spectra are composed of two subspectra ("a" and "b") with intensity ratio 2:1, reflecting the existence of two inequivalent trivalent iron sites. Subspectra "a" are assigned to the three equivalent iron atoms of the terminal Fe$_3$ units, and subspectra "b" to the three equivalent iron atoms of the central unit.

Introduction

Ferric citrate complexes play a major role in iron solubilization, transport, and utilization in animals and plants.[2] Citric acid, C(OH)(COOH)(CH₂COOH)₂, an α-hydroxy tricarboxylic acid, forms a series of stable complexes with Fe(III) ion in aqueous solution over a very large pH range (2−9), thus preventing hydrolysis of ferric ion and formation of insoluble hydroxides/oxides at physiological pH.[3] Iron levels in biological systems are controlled by citric acid chelation of Fe(III) or through redox reactions of ferric citrate.[4] In animals, including humans, bioavailability of iron is increased by citric acid, and iron citrate preparations are commercially available for use as iron supplements in foods.[5] Ever since the discovery of an iron citrate complex in plant xylem, similar complexes have been identified in a number of plants.[6] The roots of plants suffering from iron deficiency exude a fluid containing citric acid in order to extract iron from the rhizosphere. The iron citrate complexes, formed in this process, are then absorbed back into the roots and transported to the tops of the plants, where photoreduction takes place.[7] In *Escherichia coli*, ferric citrate is recognized and transferred across the cell membrane by specific regulatory membrane proteins.[8]

Thirty years ago, Saltman et al. investigated the hydrolytic polymerization of aqueous ferric citrate at pH values greater than 4.[9] It was previously reported that at such values a characteristic red-brown color appeared and that redox and glass electrode potentials became sluggish, suggesting the formation of aggregates of high nuclearities.[3d] Saltman's results in a buffer region at pH 8−9 showed the existence of very large (MW ∼2 × 10⁵, diameter 72 Å) spheres of iron hydroxide core with citrate ions bound to the surface. It was suggested that surface coverage by citrate ligands serves to protect the polymeric particles from condensing through hydroxo bridges at high pH, but no specific mode of coordination was offered.[9]

Despite the great importance of the Fe(III)−citrate system and the extensive spectroscopic and biological studies for over a century, the structures of ferric citrate complexes remained virtually unknown until recently. Two years ago we reported the syntheses, structures, and magnetic properties of two dinuclear iron(III) citrate complexes, namely, $[Fe_2(cit)_2(H_2O)_2]^{2-}$ (**1**) and $[Fe_2(Hcit)_3]^{3-}$ (**2**).[10] Complexes **1** and **2** were shown to exist in equilibrium in aqueous solution in the presence of excess citric acid. We now describe the synthesis, structure, and results of a Mössbauer spectroscopic study of an unusual, new polynuclear ferric citrate complex, namely, [Fe₉O(cit)₈-

(1) (a) Department of Inorganic and Analytical Chemistry, The Hebrew University of Jerusalem. (b) Racah Institute of Physics, The Hebrew University of Jerusalem. (c) Department of Chemistry, Massachusetts Institute of Technology.
(2) Milewska, M. J. *Z. Chem.* **1988**, *28*, 204−211.
(3) (a) Bobtelsky, M.; Jordan, J. *J. Am. Chem. Soc.* **1947**, *69*, 2886. (b) Lanford, O. E.; Quinan, J. R. *J. Am. Chem. Soc.* **1948**, *70*, 2900. (c) Warner, R. C.; Weber, I. *J. Am. Chem. Soc.* **1953**, *75*, 5086. (d) Timberlake, C. F. *J. Chem. Soc.* **1964**, 5075.
(4) (a) Guerinot, M. L.; Meidl, E. J.; Plessner, O. *J. Bacteriol.* **1990**, *172*, 3298−3303. (b) Langman, L.; Young, I. G.; Frost, G. E.; Rosenberg, H.; Gibson, F. *J. Bacteriol.* **1972**, *112*, 1142−1149.
(5) Morris, E. R. *Trace Elements in Human and Animal Nutrition*, 5th ed.; Academic Press: San Diego, CA, 1987; Chapter 4, pp 79−142.
(6) Tiffen, L. O. *Plant Physiol.* **1966**, *41*, 515.

(7) (a) Bienfait, H. F.; Scheffers, M. R. *Plant Soil* **1992**, *143*, 141−144. (b) Abrahamson, H. B.; Rezvani, A. B.; Brushmiller, J. G. *Inorg. Chim. Acta* **1994**, *226*, 117−127.
(8) (a) Frost, G. E.; Rosenberg, H. *Biochim. Biophys. Acta* **1973**, *330*, 90−101. (b) Hussein, S.; Hantke, K.; Braun, V. *Eur. J. Biochem.* **1981**, *117*, 431−437. (c) Zimmermann, L.; Hanke, K.; Braun, V. *J. Bacteriol.* **1984**, *159*, 271−277. (d) Pressler, U.; Staudenmaier, H.; Zimmermann, L.; Braun, V. *J. Bacteriol.* **1988**, *170*, 2716−2724. (e) Zhou, X. H.; van der Helm, D. *Biometals* **1993**, *6*, 37−44.
(9) (a) Spiro, T. G.; Pape, L.; Saltman, P. *J. Am. Chem. Soc.* **1967**, *89*, 5555−5559. (b) Spiro, T. G.; Bates, G.; Saltman, P. *J. Am. Chem. Soc.* **1967**, *89*, 5559−5562.
(10) Shweky, I.; Bino, A.; Goldberg, D. P.; Lippard, S. J. *Inorg. Chem.* **1994**, *33*, 5161−5162.

$(H_2O)_3]^{7-}$ (**3**), as found in the crystal of $(Hneo)_7$·**3**·neo·$61H_2O$ (**4**) (neo = neocuproine). Complex **3** consists of one planar {Fe$_3$O} unit having a structure of basic ferric carboxylate and two cuboidal {Fe$_3$O$_4$} units with a geometry which is found for the first time in a discrete complex, assembled from an aqueous solution, all of which are bridged by eight cit^{4-} ligands.

Experimental Section

Materials and General Methods. Solvents and reagents were obtained from commercial sources and used as received. Deionized water was used in the preparation of **4**. Elemental analyses (C, H, N) were performed by the Microanalyatical Services Laboratory at the Hebrew University. Iron was determined by using a Perkin-Elmer atomic absorption spectrophotometer, Model 403.

Preparation of $(Hneo)_7[Fe_9O(cit)_8(H_2O)_3]$·neo·$xH_2O$ (4). Ferric nitrate, $Fe(NO_3)_3$·$9H_2O$ (0.40 g, 1 mmol), sodium citrate, $Na_3C_6H_5O_7$·$2H_2O$ (0.29 g, 1 mmol), and neocuproine hydrate (2,9-dimethyl-1,10-phenanthroline·H_2O) (0.21 g, 1 mmol) were dissolved in 18 mL of H_2O. The solution was stirred and kept at 60 °C for 30 min. After 24 h, at room temperature, the colorless crystals of neocuproinium nitrate dihydrate were filtered and the brown-yellow filtrate was placed in a beaker and kept at 27 °C. After several days, well-developed brown crystals of **4**, suitable for X-ray diffraction studies, were obtained (yield, 15%). The crystals readily lose solvent and gradually become opaque.

Density Measurements and Elemental Analysis. The density of fresh crystals of **4** which were washed with acetonitrile was determined by flotation, in a MeCN/CCl_4 mixture. The measured density of 1.46 ± 0.01 g cm^{-3} agrees with a formula weight of 4845 and $x = 61$. Elemental analysis was carried out for crystals of **4**, washed with water, acetone, and ether. Calcd for $C_{160}H_{141}Fe_9N_{16}O_{60}$·$46H_2O$ (fw = 4579.25): C, 41.97; H, 5.09; N, 4.89; Fe, 10.98. Found: C, 41.75; H, 4.40; N, 4.99; Fe, 11.33 (AA).

Mössbauer Spectroscopy. Conventional Mössbauer spectroscopy with a 100 mCi ^{57}Co(Rh) source at room temperature and a Harwell proportional counter were used. Velocity calibration was performed with a metallic iron foil at room temperature. Isomer shifts are quoted with respect to this absorber. Measurements were performed in cryostats at 300, 90, and 4.1 K. Computer fits were performed to all measured spectra.

X-ray Crystallography. Single crystals of approximate dimensions 0.5 × 0.5 × 0.5 mm were mounted from mother liquor in a quartz capillary and mounted on a CAD4 diffractometer. Cu Kα ($\lambda = 1.5418$ Å) radiation with a graphite crystal monochromator in the incident beam was used. The unit cell dimensions were obtained by a least-squares fit of 24 reflections in the range 20° < θ < 28°. The crystals belong to the monoclinic space group $P2_1/c$. Data were measured by using an $\omega-2\theta$ motion. Due to substantial decay during data collection, four specimens were used for data acquisition in shells of 2−30°, 30−35°, 35−40°, and 40−45° in θ. The maximum value of decay, allowed for each crystal before a new crystal was used, was about 40%. Intensity data in each shell were corrected for decay, Lorentz and polarization effects, and absorption using the empirical absorption program DIFABS, incorporated into TEXSAN.[11] Individual scaling factors for each shell were refined along with the overall scaling factor. Crystallographic data and other pertinent information are given in Table 1. The heavy-atom positions were obtained by using the results of SHELX-86 direct method analysis.[12] The structure was refined to convergence, using anisotropic thermal parameters for the metal atoms and isotropic ones for all nonmetal atoms.[13] Most of the nitrogen and carbon atoms of the neocuproine groups were located from the difference Fourier maps. Their positional parameters were refined in early cycles but were kept fixed in final refinements. Only their thermal

(11) *TEXSAN: Single-Crystal Structure Analysis Software*, version 5.0; Molecular Structure Corporation: The Woodlands, TX, 1989.
(12) Sheldrick, G. M. In *Crystallographic Computing 3*; Sheldrick, G. M., Krüger, C., Goddard, R., Eds.; Oxford University Press: Oxford, 1985; p 175.
(13) All crystallographic computing was done on a VAX 9000 computer at the Hebrew University of Jerusalem.

Table 1. Crystallographic Data for $(Hneo)_7[Fe_9O(cit)_8(H_2O)_3]$·neo·$xH_2O$

empirical formula	$C_{160}H_{141}Fe_9N_{16}O_{60}$·$61H_2O$
fw	4849.43
space group	$P2_1/c$ (No. 14)
a (Å)	21.910(3)
b (Å)	25.788(5)
c (Å)	39.653(6)
β (deg)	99.47(1)
V (Å^3)	22099(7)
Z	4
T (°C)	22 ± 1
λ (Å)	1.5418
ρ_{obsd} (g cm^{-3})	1.46
ρ_{calcd} (g cm^{-3})	1.457
μ (cm^{-1})	55.35
R $(F_o)^a$	0.152
R_w $(F_o)^b$	0.179

^{a} $R = \sum||F_o| - |F_c||/\sum|F_o|$. ^{b} $R_w = [\sum w(|F_o| - |F_c|)^2/\sum|wF_o|^2]^{1/2}$.

parameters were included in the final refinement. Six atoms from the eighth neocuproine group could not be located from the maps and therefore are not included in the list of atoms. Thirty-six different sites of oxygen atoms of lattice water molecules were located from the difference maps, of which 15 were refined with a half-occupancy and two with 0.25, corresponding to $x = 27$.

Results and Discussion

Synthesis. Crystals of $(Hneo)_7$·**3**·neo·$61H_2O$ (**4**) are obtained from an aqueous solution containing equimolar quantities of ferric nitrate, sodium citrate, and neocuproine. If, however, pyridine is used instead of neocuproine, a different compound crystallizes at ~80% yield, namely, $(Hpy)_2[Fe_2(cit)_2(H_2O)_2]$·$2H_2O$.[10] The pH of both solutions is about 2.2−2.3. It is reasonable to assume that both species **1** and **3** exist in equilibrium in aqueous solution and that the two different compounds selectively crystallize depending upon which counterion is used to produce solid material. A similar phenomenon is observed in the presence of excess citric acid in which the anions of $(Hpy)_2[Fe_2(cit)_2(H_2O)_2]$·$2H_2O$ and $(Hneo)_3[Fe_2(Hcit)_3]$·nH_2O are in equilibrium in solution and selectively crystallize as a function of the counterion.[10] The relatively low yield (15%) of $(Hneo)_7$·**3**·neo·$61H_2O$ is attributed to the low solubility of $(Hneo)NO_3$·$2H_2O$ in the reaction mixture, which is removed by filtration. Attempts to produce the material by using different salts of Fe(III) failed, and the role of the nitrate ion remains unclear.

Structure. The crystal lattice of $(Hneo)_7$·**3**·neo·$61H_2O$ contains one large anionic complex of **3** in which all nine iron atoms are in the 3+ oxidation state, *vide infra*, and all eight citrate ligands are fully deprotanated, utilizing the alkoxide and three carboxylate ends for coordinating metal atoms. The overall charge of the complex is therefore 7−. There are eight neocuproine groups in the lattice, seven of which are assigned to be 1+ neocuproinium (Hneo) ions and one as a neutral neocuproine molecule. The eight planar neocuproine units are stacked in the crystal in an infinite chain propagating parallel to the principal axes of the cylindrical complex **3**, with an average distance of 3.5 Å between the ring planes. It is assumed that the cocrystallization of an additional neutral neo molecule facilitates a continuous stacking which stabilizes the crystal lattice. In addition, the lattice contains about 61 water molecules of crystallization (as deduced from the density measurements), of which only 27 were located in the X-ray study. This discrepancy is attributed to an extensive disorder in the hydrogen-bonding network and to the limits of the resolution of the data. The water molecules which were located and

Table 2. Positional Parameters of Significant Atoms in **3**

atom	x	y	z
Fe(1)	0.2999(3)	0.9472(2)	0.2288(1)
Fe(2)	0.3519(3)	0.8568(2)	0.1842(1)
Fe(3)	0.2836(3)	0.8262(2)	0.2490(1)
Fe(4)	0.0549(3)	0.8143(2)	0.1582(1)
Fe(5)	0.1088(3)	0.8687(2)	0.0970(1)
Fe(6)	0.0629(3)	0.9423(2)	0.1545(1)
Fe(7)	0.5792(3)	0.8493(2)	0.2738(2)
Fe(8)	0.5118(3)	0.8458(3)	0.3405(1)
Fe(9)	0.5379(3)	0.9564(2)	0.3084(2)
O(1)	0.3114(9)	0.8746(7)	0.2207(4)
O(1W)	0.286(1)	1.0259(8)	0.2375(5)
O(2W)	0.399(1)	0.8354(8)	0.1449(5)
O(3W)	0.249(1)	0.7732(7)	0.2813(5)
O(11)	0.307(1)	0.8690(8)	0.2939(5)
O(12)	0.3430(8)	0.9401(7)	0.2793(4)
O(13)	0.473(1)	0.9128(8)	0.3255(5)
O(15)	0.500(1)	0.864(1)	0.3870(7)
O(16)	0.468(1)	1.0067(9)	0.3073(5)
O(21)	0.427(1)	0.8996(8)	0.2006(5)
O(22)	0.386(1)	0.9699(7)	0.2172(5)
O(23)	0.534(1)	0.9209(8)	0.2649(5)
O(24)	0.587(1)	1.014(1)	0.2914(6)
O(26)	0.564(1)	0.8514(8)	0.2239(5)
O(31)	0.365(1)	0.7896(7)	0.2600(5)
O(32)	0.393(1)	0.7961(7)	0.2081(5)
O(33)	0.512(1)	0.8185(7)	0.2921(5)
O(34)	0.616(1)	0.7819(9)	0.2711(5)
O(36)	0.450(1)	0.7919(9)	0.3391(5)
O(41)	0.315(1)	0.9145(7)	0.1521(5)
O(42)	0.2564(9)	0.9588(7)	0.1807(5)
O(43)	0.1336(9)	0.9292(7)	0.1287(4)
O(44)	0.110(1)	0.9148(8)	0.0579(5)
O(46)	0.120(1)	1.0005(7)	0.1668(5)
O(51)	0.194(1)	0.8570(7)	0.2410(4)
O(52)	0.2178(9)	0.9403(7)	0.2436(4)
O(53)	0.0799(8)	0.8855(7)	0.1866(4)
O(55)	0.005(1)	0.9677(8)	0.1854(5)
O(56)	0.068(1)	0.7876(7)	0.2060(5)
O(61)	0.2537(9)	0.7790(7)	0.2103(5)
O(62)	0.2784(9)	0.8123(7)	0.1631(4)
O(63)	0.1275(9)	0.8160(7)	0.1357(4)
O(65)	0.037(1)	0.742(1)	0.1425(7)
O(66)	0.185(1)	0.8383(8)	0.0887(5)
O(71)	0.057(1)	0.8216(8)	0.0660(5)
O(73)	0.0291(9)	0.8788(7)	0.1204(4)
O(75)	0.019(1)	0.9862(8)	0.1191(5)
O(76)	−0.034(1)	0.8108(8)	0.1519(5)
O(81)	0.568(1)	0.978(1)	0.3515(7)
O(83)	0.586(1)	0.8863(8)	0.3248(5)
O(84)	0.574(1)	0.796(1)	0.3616(7)
O(86)	0.663(1)	0.873(1)	0.2797(6)

Table 3. Important Bond Distances (Å) and Angles (deg) in **3**

atoms	distance	atoms	distance
Fe(1)−Fe(2)	3.243(8)	Fe(4)−O(73)	2.25(2)
Fe(1)−Fe(3)	3.256(8)	Fe(5)−O(43)	2.02(2)
Fe(2)−Fe(3)	3.276(8)	Fe(5)−O(63)	2.04(2)
Fe(4)−Fe(5)	3.196(8)	Fe(5)−O(73)	2.13(2)
Fe(4)−Fe(6)	3.310(7)	Fe(6)−O(43)	2.02(2)
Fe(5)−Fe(6)	3.254(8)	Fe(6)−O(53)	1.93(2)
Fe(7)−Fe(8)	3.24(1)	Fe(6)−O(73)	2.17(2)
Fe(7)−Fe(9)	3.275(9)	Fe(7)−O(23)	2.10(2)
Fe(8)−Fe(9)	3.21(1)	Fe(7)−O(33)	1.91(2)
Fe(1)−O(1)	1.92(2)	Fe(7)−O(83)	2.22(2)
Fe(1)−O(1W)	2.09(2)	Fe(8)−O(13)	1.97(2)
Fe(2)−O(1)	1.87(2)	Fe(8)−O(33)	2.05(2)
Fe(2)−O(2W)	2.08(2)	Fe(8)−O(83)	2.11(3)
Fe(3)−O(1)	1.85(2)	Fe(9)−O(13)	2.01(2)
Fe(3)−O(3W)	2.10(2)	Fe(9)−O(23)	1.94(2)
Fe(4)−O(53)	2.18(2)	Fe(9)−O(83)	2.14(2)
Fe(4)−O(63)	1.95(2)		

atoms	angle	atoms	angle
O(53)−Fe(4)−O(63)	93.6(8)	O(23)−Fe(9)−O(83)	79.6(8)
O(53)−Fe(4)−O(73)	74.6(6)	Fe(1)−O(1)−Fe(2)	117(1)
O(63)−Fe(4)−O(73)	79.2(8)	Fe(1)−O(1)−Fe(3)	119(1)
O(43)−Fe(5)−O(63)	92.6(7)	Fe(2)−O(1)−Fe(3)	123(1)
O(43)−Fe(5)−O(73)	77.7(8)	Fe(8)−O(13)−Fe(9)	108(1)
O(63)−Fe(5)−O(73)	80.2(8)	Fe(7)−O(23)−Fe(9)	108.4(9)
O(43)−Fe(6)−O(53)	97.2(8)	Fe(7)−O(33)−Fe(8)	110(1)
O(43)−Fe(6)−O(73)	76.7(7)	Fe(5)−O(43)−Fe(6)	107.2(9)
O(53)−Fe(6)−O(73)	81.2(7)	Fe(4)−O(53)−Fe(6)	107.1(8)
O(23)−Fe(7)−O(33)	93.5(9)	Fe(4)−O(63)−Fe(5)	106.4(9)
O(23)−Fe(7)−O(83)	74.6(8)	Fe(4)−O(73)−Fe(5)	93.9(7)
O(33)−Fe(7)−O(83)	76.9(8)	Fe(4)−O(73)−Fe(6)	96.9(7)
O(13)−Fe(8)−O(33)	94.9(8)	Fe(5)−O(73)−Fe(6)	98.4(8)
O(13)−Fe(8)−O(83)	78(1)	Fe(7)−O(83)−Fe(8)	96.7(9)
O(33)−Fe(8)−O(83)	76.7(8)	Fe(7)−O(83)−Fe(9)	97.4(8)
O(13)−Fe(9)−O(23)	96.2(9)	Fe(8)−O(83)−Fe(9)	98.(1)
O(13)−Fe(9)−O(83)	76.3(9)		

bridged "basic" iron carboxylate in which the three Fe(III) ions are coordinated to six bridging $RCOO^-$ groups from different citrate ligands. In addition, each iron atom is coordinated to an H_2O ligand, completing a slightly distorted octahedral geometry.

The two terminal Fe_3 units possess a "voided cubane" structure with a cuboidol $\{Fe_3O_4\}$ core, as shown in Figure 3. The three Fe(III) ions form an idealized equilateral triangle and are bridged by a μ_3-oxygen atom of an alkoxo group from a capping citrate. The other three coordination positions of each iron atom are occupied by terminal carboxylate groups from three different citrates, one from the capping citrate and two from two different bridging citrates, completing slightly distorted coordination spheres.

A discrete $\{Fe_3O_4\}$ unit is very rare in the chemistry of iron-(III) and was only recently reported for the first time in the structure of $K[Fe_3(OCH_3)_7(dbm)_3]\cdot4CH_3OH$ (Hdbm = dibenzoylmethane).[14] This compound was obtained from a strongly alkaline methanolic solution of $FeCl_3$ and Hdbm. The metal atoms in this structure are bridged by alkoxo μ_3-OCH_3 and μ_2-OCH_3 groups and coordinated to a bidentate dbm ligand and a terminal CH_3O^- ligand. A comparison between the average bond lengths and angles in **3** and in $[Fe_3(OCH_3)_7(dbm)_3]^-$ is given in Table 4, from which it is evident that the dimensions of the $\{Fe_3O_4\}$ cores in both compounds are very similar within the experimental error.

In both compounds, the oxygen atoms of the M_3O_{13} unit lie in two approximately parallel layers (Figure 3) in an approximate

refined are engaged in an extensive hydrogen-bonding network involving water, terminal citrate oxygen atoms of **3**, and the neocuproinium nitrogen atoms.

The atomic positional parameters of the significant atoms in **3** are listed in Table 2, and Table 3 presents the important bond lengths and angles. Figure 1 shows the structure and the numbering scheme of **3**, and Figure 2 presents a stereoview of the complex.

With $Z = 4$ in the cell of space group $P2_1/c$, there is no crystallographic symmetry imposed upon the complex. The polynuclear anion $[Fe_9O(cit)_8(H_2O)_3]^{7-}$ consists of three parallel triangular Fe_3 units which form a slightly distorted trigonal prism. The two terminal units in this molecular "ferric triple-decker" are connected by three bridging tetradentate cit^{4-} ligands to the central one, and each of the two terminal Fe_3 units is capped by another tetradentate cit^{4-} ligand. The Fe_3 units are separated by approximately 5.6 Å along the pseudo-3-fold axis. The central triiron unit has the structure of the well-known oxo-

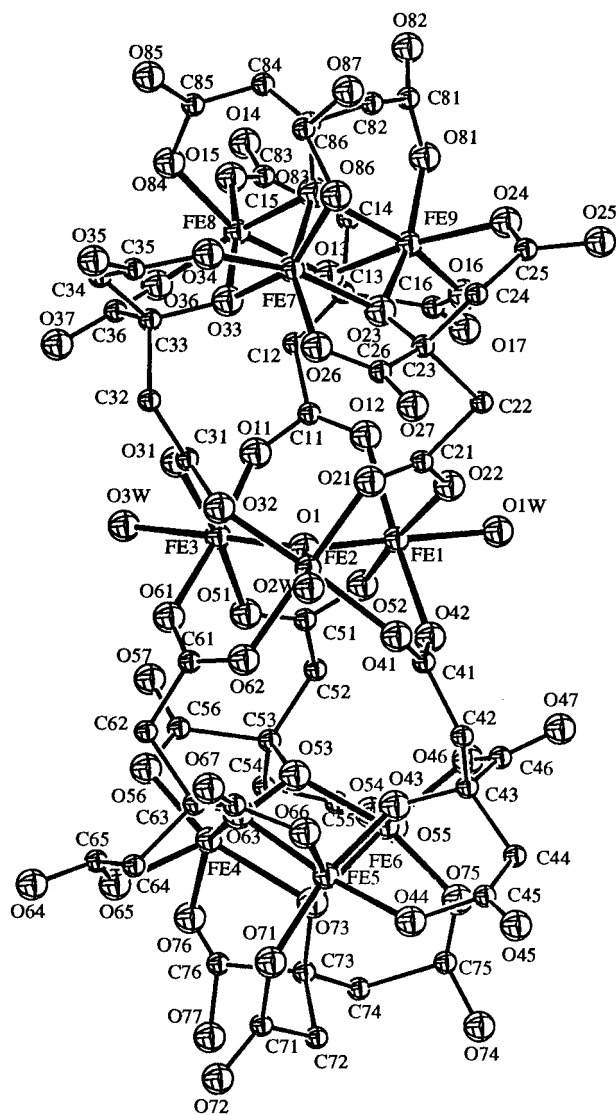(14) Caneschi, A.; Cornia, A.; Fabretti, A. C.; Gatteschi, D.; Malavasi, W. *Inorg. Chem.* **1995**, *34*, 4660−4668.

Figure 1. Structure of $[Fe_9O(cit)_8(H_2O)_3]^{7-}$.

Figure 2. Stereoview of $[Fe_9O(cit)_8(H_2O)_3]^{7-}$.

Figure 3. $\{Fe_3O_4\}$ unit as found in **3**.

Table 4. Average Bond Distances (Å) and Angles (deg) in the $\{Fe_3O_4\}$ Core in **3** and $[Fe_3(OCH_3)_7(dbm)_3]^-$

complex	**3**[a]	$[Fe_3(OCH_3)_7(dbm)_3]^-$
Fe···Fe[b]	3.25[2][c]	3.242[1]
Fe$-\mu_3$-O	2.17[2]	2.144[6]
Fe$-\mu_2$-O	2.01[2]	2.005[5]
Fe$-\mu_3$-O$-$Fe	98[1]	98.3[1]
Fe$-\mu_3$-O$-$Fe	108[1]	107.9[4]

[a] Equivalent parameters from the two Fe_3O_4 units in **3** were averaged. [b] An ideal C_{3v} symmetry is assumed. [c] Numbers in brackets are grand average values obtained by the expression $[(\sum\Delta_i^2)/n(n-1)]^{1/2}$.

plane of the second Fe_3O_{13} unit are in the range 0.11−0.14 Å. For comparison, in $[Fe_3(OCH_3)_7(dbm)_3]^-$ these deviations are 0.14 and 0.23 Å for the respective planes.[14] These differences can be explained by the different constraints imposed by the chelating citrates and the dbm ligands.

Complex **3** presents the first example in which an Fe_3O_{13} unit is assembled in an aqueous solution and exists in a discrete complex. Similar *cp* Fe_3O_{13} cores exist, however, in several compounds as part of extended arrays in higher iron aggregates.[15]

Another interesting aspect of **3** is the mode of coordination of the citrate ligands, which cap the two terminal Fe₃ units. Binding to all three metal atoms is accomplished by formation of a μ_3-O(alkoxo) cap and coordination of each of the three carboxylato groups to a different iron atom in the Fe₃ system. Such a mode of coordination may serve as a model for the binding of citrate ligands to the surface of very large polymetallic assemblies.[10]

Mössbauer Spectroscopy. The spectra at 300 and 90 K revealed one apparent symmetric doublet, but efforts to fit these spectra with just one doublet of Lorentzian line shape gave a

(15) (a) Heath, S. L.; Powell, A. K. *Angew. Chem., Int. Ed. Engl.* **1992**, *31*, 191. (b) Taft, K. L.; Caneschi, A.; Pence, L. E.; Delfs, C. D.; Papaefthymiou, G. C.; Lippard, S. J. *J. Am. Chem. Soc.* **1993**, *115*, 11753. (c) Boone, S. R.; Purser, G. H.; Chang, H.-R.; Lowery, M. D.; Hendrickson, D. N.; Pierpont, C. G. *J. Am. Chem. Soc.* **1989**, *111*, 2292. (d) Nair, V. S.; Hagen, K. S. *Inorg. Chem.* **1992**, *31*, 4048. (e) Shoner, S. C.; Power, P. P. *Inorg. Chem.* **1992**, *31*, 1001. (f) Taft, K. L.; Papaefthymiou, G. C.; Lippard, S. J. *Science* **1993**, *259*, 1302. (g) Caneschi, A.; Cornia, A.; Fabretti, A. C.; Gatteschi, D. *Angew. Chem., Int. Ed. Engl.* **1995**, *34*, 2716. (h) Hegetschweiler, K.; Schmalle, H.; Streit, H. M.; Schneider, W. *Inorg. Chem.* **1990**, *29*, 3625. (i) Taft, K. L.; Papaefthymiou, G. C.; Lippard, S. J. *Inorg. Chem.* **1994**, *33*, 1510. (j) Hegetschweiler, K.; Schmalle, H. W.; Streit, H. M.; Gramlich, V.; Hund, H.-U.; Erni, I. *Inorg. Chem.* **1992**, *31*, 1299.

closest-packing (*cp*) geometry. In complex **3**, the average deviations from the best planes through atoms O(73), O(65), O(76), O(71), O(44), O(75) and O(55) and from the equivalent plane of the second Fe_3O_{13} unit are about 0.39 Å. The average deviations from the second set of planes, defined by O(63), O(53), O(43), O(46), O(56), and O(66), and from the equivalent
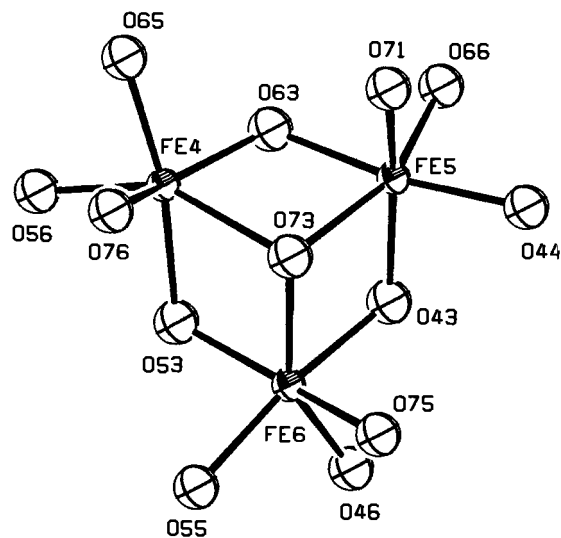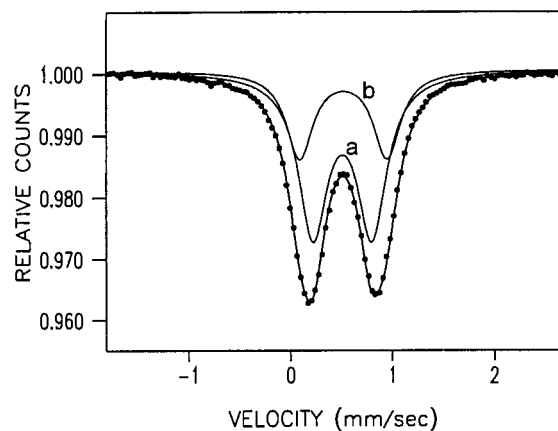
Figure 4. Mössbauer spectrum of **1** at 90 K. The spectrum is composed of subspectra "a" and "b" with intensity ratio 2:1. Least-squares fits to the experimental data were done using Mössbauer parameters listed in Table 5. See text for discussion of fitting procedure.
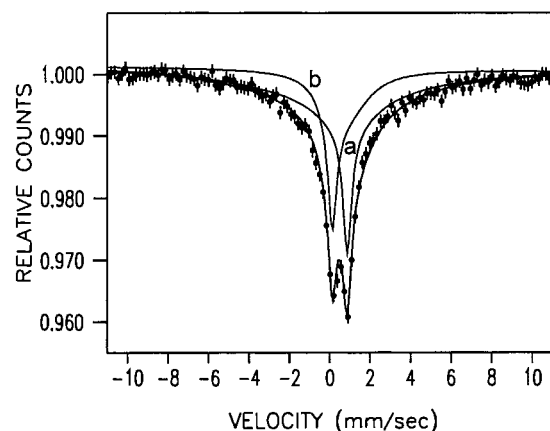
Table 5. Mössbauer Parameters for **3**

temp (K)	site	rel int	line width (mm/s)	Δ (mm/s)	δ^a (mm/s)	relax. time (ns)	H_{eff} (kOe)
300	"a"	2	0.33(1)	0.54(1)	0.40(1)		
	"b"	1	0.29(1)	0.78(2)	0.41(1)		
90	"a"	2	0.33(1)	0.57(1)	0.50(1)		
	"b"	1	0.29(1)	0.84(1)	0.51(1)		
4.1	"a"	2	0.26	−0.58	0.55	0.79	55
	"b"	1	0.35	+0.82	0.53	0.20	55

^{a} Isomer shifts δ are relative to metallic iron at room temperature.

very poor χ^2. The computer fit was much improved when two doublets with an intensity ratio of 2:1 were introduced. Figure 4 displays the spectrum obtained at 90 K, and the parameters obtained from the computer fits are summarized in Table 5. These parameters are characteristic of trivalent, high-spin iron. The increase of isomer shift at lower temperature is consistent with a second-order Doppler shift. The spectrum obtained at 4.1 K, shown in Figure 5, is asymmetric and extends to much higher velocities. Its shape is characteristic of relaxation phenomena[16] and cannot be fitted with doublets, or with one relaxation spectrum. Very good computer fits can be obtained by using two inequivalent sites with quadrupole splittings (Δ) constrained to be identical to those found at 90 K and a simple relaxation model with different relaxation times at the two sites. A hyperfine field of 55 T, characteristic for trivalent iron, was assumed in the fits. The quadrupole splittings of the two sites have opposite signs, the obtained parameters being given in Table 5. As can be seen from the table, the relaxation times of

Figure 5. Mössbauer parameters of **1** at 4.1 K. The spectrum is composed of relaxation subspectra "a" and "b". Least-squares fits to the experimental data were done using Mössbauer parameters listed in Table 5.

the two sites differ, showing faster relaxation in site "b". All the quadrupole splittings and isomer shifts observed are within the range observed for trinuclear iron carboxylates.[17]

Consistent with the crystal structure, subspectrum "a" is assigned, with relative intensity 2, to the three iron atoms of the terminal Fe_3 units and subspectrum "b", with relative intensity 1, to the three iron atoms of the central triiron unit. Within each of these units, the three iron atoms are identical. The quadrupole splitting in site "a" is smaller than in site "b" and, as can be deduced from the relaxation spectra observed at 4.1 K, the sign of the electric field gradient is opposite in the two sites and negative in site "a". The somewhat faster relaxation observed in site "b" may point to stronger magnetic coupling between the iron atoms in this site. This observation is in agreement with the measured J values for "basic" iron carboxylates (typical values 60 cm^{-1})[18] and for $\{Fe_3O_4\}$ in $[Fe_3(OCH_3)_7(dbm)_3]^-$ (8.7 cm^{-1}).[14]

Supporting Information Available: Tables of complete atomic positional and thermal parameters, bond lengths and angles, and least-squares planes, a packing diagram of **4**, and a figure showing the labeling scheme of the neocuproine groups (34 pages). Ordering information is given on any current masthead page.

(16) Wickman, H. H.; Wertheim, G. K. In *Chemical Applications of Mössbauer Spectroscopy*; Goldanskii, V. I., Herber, R. H., Eds.; Academic Press: San Diego, CA, 1968; p 548.

(17) Long, G. J.; Robinson, W. T.; Tappmeyer, W. P.; Bridges, D. L. *J. Chem. Soc., Dalton Trans.* **1973**, 573.

(18) (a) Gorun, S. M.; Lippard, S. J. *J. Am. Chem. Soc.* **1985**, *107*, 4568. (b) Gorun, S. M.; Papaefthymiou, G. C.; Frankel, R. B.; Lippard, S. J. *J. Am. Chem. Soc.* **1987**, *109*, 4244.